Thermal Magnetoresistance of Zinc at Low Temperatures*

Perry B. Alers

U. S. Naval Research Laboratory, Washington, D. C., and University of Maryland, College Park, Maryland

(Received September 26, 1955)

The variation of the low-temperature thermal resistance of single crystals of zinc in large magnetic fields has been investigated. The work was divided into two parts, one using very large fields ($H \leqslant 60$ kilogauss) and the other using fields ranging to 25 kilogauss. The high-field work was concerned mostly with the behavior of the thermal magnetoresistance for various orientations of the crystalline axes relative to the magetic field. It was found that the thermal magnetoresistance is a strong function of orientation in the field, and an attempt was made to extrapolate the data obtained to infinite fields. The low-field work was carried out primarily to investigate the de Haas Alphen effect, and electrical as well as thermal magnetoresistance data were taken. Oscillations of the de Haas-van Alphen type were found in both the thermal and the electrical magnetoresistance and an average value of $\beta^*/E_0 = 5.8 \times 10^{-5}$ gauss^{-1} was derived from the thermal data. Comparison with theory yielded a value of the order of 0.2 electron per atom for both the thermal and electrical cases. The variation of the Lorenz ratio with magnetic field was also derived.

INTRODUCTION

THE effect of a magnetic field on the thermal conductivity of metals at low temperatures has been investigated sporadically for the past twenty years. Much of the work, however, has been done at the temperature of liquid hydrogen (14°K to 20°K), and extension to the liquid helium range is a fairly recent development.[1]

The first work done at 4.2°K was done by Shalyt[2] in 1944 in which he investigated the thermal magnetoresistance of bismuth. In 1950, Hulm,[3] in connection with his work on the thermal conductivity of superconductors, investigated the behavior of tin monocrystals in fields ranging to 1500 gauss. His crystals were quite pure and the magnetoresistance effects were strong, but the observations were incidental to the main work on superconductivity. In 1953, a survey of thermal magnetoresistance by Mendelssohn and Rosenberg[4] was carried out on a variety of metals, many of them single crystals. They were primarily interested in testing the validity of Kohler's rule[5] for thermal resistance. They used fields up to 4 kG for most of the work, but the data for Zn, Cd, Sn, and Tl were carried to 20 kG. However, a detailed investigation of the properties of any particular metal was not carried out.

We were interested in the behavior of the thermal magnetoresistance because of the recent observation that the peculiar behavior of the diamagnetic susceptibility of certain metals (the de Haas-van Alphen effect) is reflected in other physical properties. Work has been done on the electrical magnetoresistance,[6] Hall effect,[7] and thermal emf[8] of several metals, and a similar investigation of the thermal conductivity seemed to be in order. Since the experiments reported here were undertaken, work has been done on bismuth by Steele and Babiskin[9] on nearly all of these properties. In addition, the availability of large magnetic fields made such work desirable. The theoretical description of low-temperature magnetoresistive effects is not in a satisfactory state and one of the reasons is the scarcity of experimental data. Experiments in high fields can provide such data over an extended range, especially if more than one temperature is used.

The work reported here was therefore undertaken to make a thorough investigation of the effect of magnetic fields on the thermal magnetoresistance of crystals of zinc at various orientations and at two different temperatures. The work fell into two categories. First, the high-field ($H \leqslant 60$ kilogauss) measurements were made on crystals of various orientations with respect to the magnetic field. Second, the low-field ($H \leqslant 25$ kilogauss) measurements were made to investigate the existence of de Haas-van Alphen behavior in both the thermal and electrical magnetoresistance. The associated electrical measurements allowed us to observe the behavior of the Lorenz ratio as a function of field and to make a crude estimate of the heat conductivity of the lattice.

* Based on a thesis submitted to the Faculty of the Graduate School of the University of Maryland in partial fulfillment of the requirements for the degree of Doctor of Philosophy (unpublished).

[1] J. L. Olsen and H. M. Rosenberg, Advances in Phys. 2, 28 (1953). This is a review article on low-temperature thermal conductivity containing a bibliography complete to about the middle of 1952.

[2] S. Shalyt, J. Phys. (U.S.S.R.) 8, 315 (1944).

[3] J. K. Hulm, Proc. Roy. Soc. (London) 204, 98 (1950).

[4] K. Mendelssohn and H. M. Rosenberg, Proc. Roy. Soc. (London) 218, 190 (1953).

[5] M. Kohler, Naturwiss. 36, 186 (1949).

[6] Bi: P. B. Alers and R. T. Webber, Phys. Rev. 91, 1060 (1953); Zn: T. G. Berlincourt and J. K. Logan, Phys. Rev. 93, 348 (1954), using data of N. M. Nachimovitch, J. Phys. U.S.S.R. 6, 111 (1942); C (graphite): T. G. Berlincourt and J. K. Logan, Phys. Rev. 93, 348 (1954); Sb: M. C. Steele, Phys. Rev. 98, 1180(A) (1955).

[7] Bi: Reynolds, Leinhardt, Hemstreet, and Triantos, Phys. Rev. 96, 1203 (1954); L. C. Brodie, Phys. Rev. 93, 935 (1954); C (graphite): T. G. Berlincourt and M. C. Steele, Phys. Rev. 98, 227(A) (1955). Sb: M. C. Steele, Phys. Rev. 98, 1180(A) (1955).

[8] Bi: M. C. Steele and J. Babiskin, Phys. Rev. 94, 1394 (1954).

[9] Bi: M. C. Steele and J. Babiskin, Phys. Rev. 98, 359 (1955).

APPARATUS

The calorimeter[10] for the high-field work was designed to fit into a metal dewar flask, suitable for use in a Bitter-type solenoid magnet. The calorimeter can was $2\frac{1}{8}$ in. in diameter and $2\frac{7}{8}$ in. high and was turned out of a solid piece of brass. See Fig. 1. It was secured to a brass lid by means of twelve beryllium-copper screws, and a gold-wire ring provided a vacuum seal. The crystal to be investigated was mounted perpendicular to the axis of this can, with one end soldered to a copper post in thermal contact with the helium bath. A small heater coil, noninductively wound, was attached to the other end of the specimen, and three carbon-composition resistors used as thermometers were attached to the specimen rod at appropriate points. Two of these resistors were used to give the temperature difference, and the third monitored the average temperature of measurement.

The entire assembly was attached to a stainless steel pumping line leading to a vacuum system mounted on the top plate of the apparatus. The plate was screwed to a flange on the top of the metal dewar flask. An O-ring seal at this point made the dewar system vacuum tight and allowed us to reduce the temperature by pumping on the helium bath.
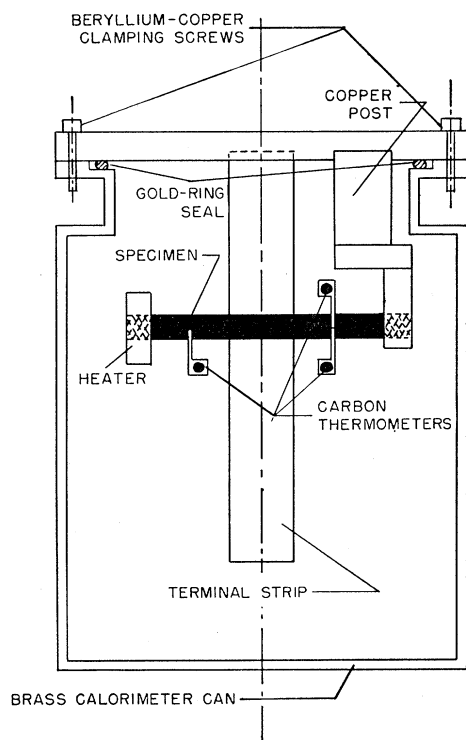
The low-field apparatus was the same in principle, but since the magnetic field was horizontal, the specimen could be mounted vertically. The gap between the magnet pole pieces was $1\frac{5}{8}$ in., but the available space at liquid helium temperatures, after the dewar flasks were assembled, was only $\frac{1}{2}$ in. in diameter. Accordingly, a new calorimeter was designed, as shown in Fig. 2.

Temperature differences of the order of a few hundredths of a degree Kelvin were used, and they were derived from a measurement of the difference between the resistance of the two carbon thermometers. A comparison circuit was used to measure this difference directly. It is fully described in an article by Dauphinee[11] except that the motor-driven switch employed in that design was replaced by a high-speed double-pole-double-throw switch in the form of a "Millisec" relay driven by a square-wave generator. Such a circuit provided greater sensitivity than a Wheatston bridge at the power levels employed ($<1\mu w$), while permitting the use of a conventional deflection galvanometer of moderate sensitivity.

The specimens used came from two different sources. For the high-field work, crystals grown by Horizons, Inc., Cleveland, Ohio, were used. In Zn I and Zn II the hexagonal axis was nearly perpendicular to the axis of the rod ($\varphi = 89°$), and in Zn III the axis was parallel. The low-field work was done using crystals very kindly loaned to us by Dr. E. I. Salkovitz of this laboratory. In both crystals the hexagonal axis was perpendicular to the rod axis; in Zn VI, $\varphi = 89°$ and in Zn VII, $\varphi = 85°$.

FIG. 1. Diagram of calorimeter used for high-field work.

[10] Many of the techniques employed in the design of these calorimeters were originated or adapted by D. A. Spohr of this laboratory, now on leave at the Clarendon Laboratory, Oxford, England.
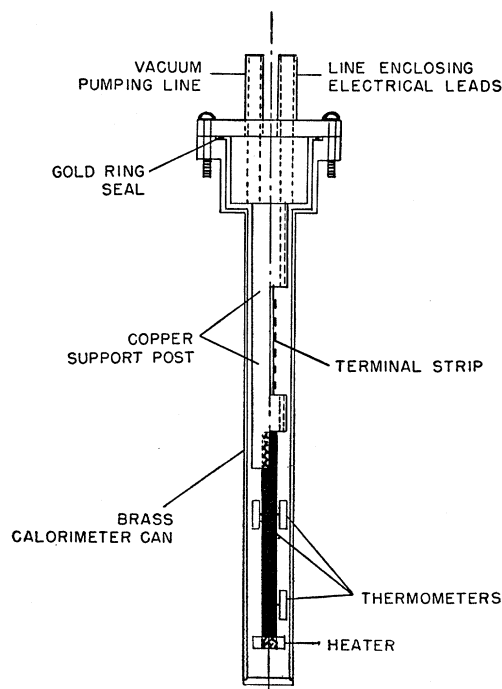

FIG. 2. Diagram of calorimeter used for low-field work.

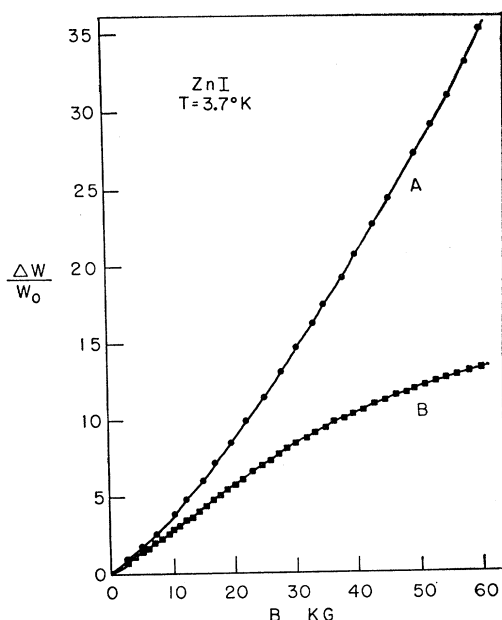[11] T. M. Dauphinee, Can. J. Phys. 31, 577 (1953).

FIG. 3. Relative change in thermal resistance (W) as a function of magnetic field for Zn I. Heat flow is perpendicular to the field and perpendicular to the hexagonal axis of the crystal. For curve A, the hexagonal axis is at an angle of about 5° with the direction of the field. For curve B, the hexagonal axis is parallel to the field.

The thermal and electrical constants of each crystal are given in Table I.

EXPERIMENTAL RESULTS

The thermal magnetoresistance data is presented in terms of the relative change in thermal resistance $\Delta W/W_0$. W_0 is the thermal resistance in zero field at the temperatures indicated on the graphs, and $\Delta W = W - W_0$, the change in thermal resistance as the field is increased. Values of W_0 for each crystal at the temperatures employed are given in Table I.

High-Field Results

Using Zn I, two sets of data were obtained. In both cases, the heat current $\dot{Q}$ flowed perpendicular to the hexagonal axis of the crystal, but in one run the hexagonal axis was not quite parallel ($\sim 5°$ off) to the magnetic field. This is shown as curve A in Fig. 3. The orientation was then adjusted and the data for curve B were obtained. It is clear that the thermal magnetoresistance is a very strong function of orientation.

In Zn II, the crystal was oriented in the apparatus so that the magnetic field was perpendicular to the hexagonal axis. The heat current, $\dot{Q}$, was also perpendicular to this axis, as before. The data for two temperatures appear in the lower curves of Fig. 4. A crystal of different orientation was used for Zn III in order to obtain the third permutation of $\dot{Q}$, H, and crystal axis. In this crystal the field was perpendicular to the hexagonal axis, but the heat current was parallel to it. The data obtained appear in the upper curves of Fig. 4.

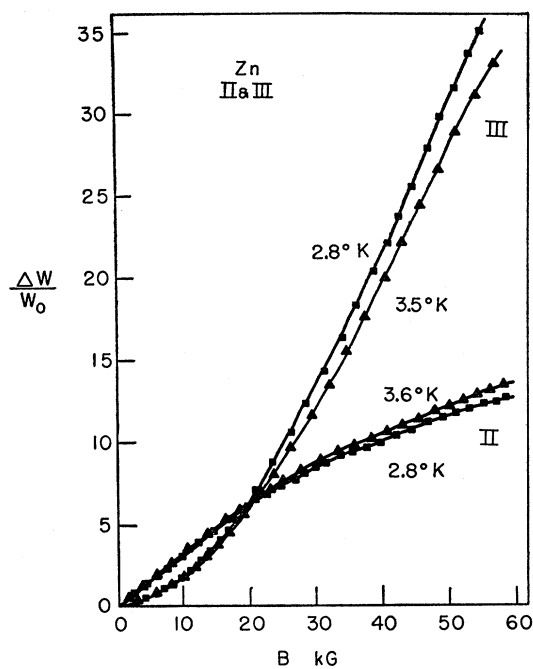In both cases, the temperature dependence of the

FIG. 4. Relative change in thermal resistance (W) as a function of magnetic field for Zn II and Zn III. For Zn II, the heat flow is perpendicular to the field and perpendicular to the hexagonal axis of the crystal. For Zn III, the heat flow is perpendicular to the field and parallel to the hexagonal axis of the crystal. In both cases, the hexagonal axis is perpendicular to the field.

magnetoresistive effects was small. However, the effect of a change of temperature on Zn II was opposite to that on Zn III. This may or may not be a real effect; it is felt that there is probably an error in the value of W_0.

As a general rule, the magnetic effects were smaller in the case where the crystal presented a high degree of symmetry to the field. This was true for Zn I (B) and Zn II. In the case of Zn III, the positions of the binary axes were not known, but since it is unlikely that they were precisely parallel or perpendicular to the field, the strong effects observed should not be unexpected. This dependence on symmetry is recognized in most theories of electrical magnetoresistance, and these results can be looked upon as corroboration of the effect in the thermal analog.

It is therefore plausible to assume that the orientations of highest symmetry would be the ones most sensitive to small changes, and it appears that this is true. When the field is parallel to the hexagonal axis, a marked de Haas-van Alphen effect is observed in the susceptibility, and it is also at this orientation that anomalies in the electrical magnetoresistance have appeared.[6] It was thus an orientation of considerable interest for the thermal magnetoresistance.

Low-Field Results

The work at low fields was carried out using a horizontal iron-core magnet which could be rotated about
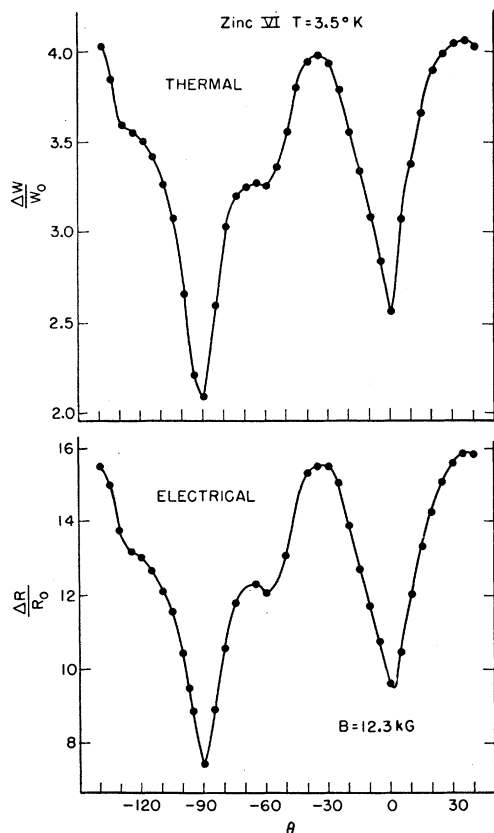
FIG. 5. Comparison of thermal and electrical magnetoresistance as a function of angle for field fixed at 12.3 kG.
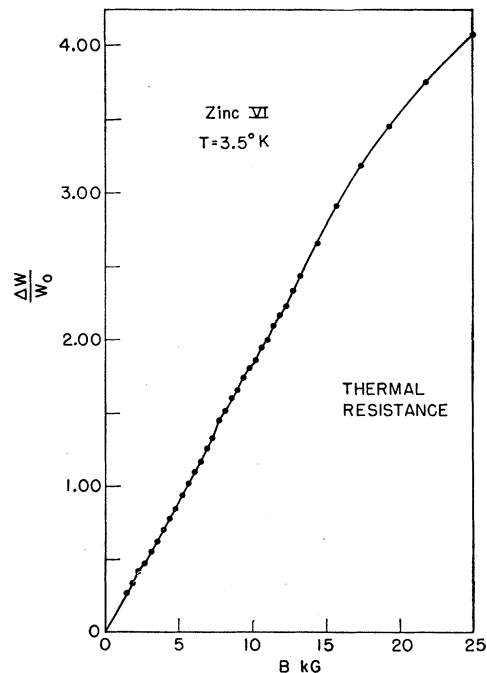

FIG. 6. Relative change in thermal resistance as a function of field for Zn VI. Hexagonal axis is perpendicular to heat flow and parallel to field direction.

a vertical axis. The magnet was calibrated by means of a nuclear resonance fluxmeter, and it could be positioned with respect to the crystalline axes of the specimen with a high degree of precision. It was therefore well-suited to an investigation of de Haas-van Alphen behavior.

Both thermal and electrical magnetoresistance data were taken on the specimens used in this part of the work. The characteristics of Zn VI and Zn VII appear in Table I. In both specimens, the hexagonal axis was perpendicular to the rod axis, and thus lay in the horizontal plane, making an angle θ with the field direction. To insure proper orientation of the field with respect to the crystalline axes, a "rotation diagram" consisting of the variation of the magnetoresistance with the angular position of the magnet was taken at some constant field

—in this case, about 12 kG. Both the electrical and thermal cases were studied, and the data for Zn VI appear in Fig. 5. There is clearly strong similarity between the two curves, which would imply that the thermal conduction is almost entirely electronic.

The absolute minimum in the curves corresponds to the orientation for which the field is perpendicular to the hexagonal axis ($\theta = 90°$) and the relative minimum occurs when the field is parallel to the axis ($\theta = 0°$). It is this orientation for which the de Haas-van Alphen effect is the strongest. Accordingly, the magnet was locked into position, and the variation with field for both the thermal and electrical magnetoresistance was observed. The resulting curves, for Zn VI, appear in Figs. 6 and 7.

Again, the electrical and thermal curves resemble each other closely, and there is a faint suggestion of an oscillatory component on each one of them. By subtracting away the gross increases in resistance, it is found that the oscillations are periodic in reciprocal

TABLE I. Electrical and thermal characteristics of the zinc crystals used in these experiments.

	T °K	K_0 watt-units	σ_0 ohm^{-1} cm^{-1}	L_0 watt-ohm/(°K)^2	l/A cm^{-1}
Zn I	3.75	6.50	...	...	19.8
Zn II	3.58	7.34	...	...	17.9
Zn III	3.50	6.12	...	...	17.7
Zn VI	3.45	5.60	1.23×10^8	1.32×10^{-8}	21.6
Zn VII	3.46	4.78	1.00×10^8	1.38×10^{-8}	24.5

TABLE II. Values of the de Haas-van Alphen parameter β^*/E_0 derived from thermal and electrical magnetoresistance data, compared to the value obtained from susceptibility measurements

		β^*/E_0, gauss^{-1}
Zn VI	Thermal	5.7×10^{-5}
	Electrical	5.3×10^{-5}
Zn VII	Thermal	6.0×10^{-5}
	Electrical	5.8×10^{-5}
Zn	Susceptibility	6.4×10^{-5}

field, a characteristic of the de Haas-van Alphen effect. The results of this type of analysis appear as Fig. 8. Since only two oscillations are clearly observed, the de Haas-van Alphen parameter, β^*/E_0, derived from the oscillations can be used only for purposes of comparison.

Following the assumption that the oscillatory component of the thermal magnetoresistance is simply added to a steady monotonic increase, we can write

$$\Delta W/W_0 = A_1(H,T) + A_2 \sin(2\pi E_0/\beta^* H).$$

In this expression $\beta^* = eh/m^*c$, a double effective Bohr magneton, and E_0 is the energy overlap between the Brillouin zone boundary and the Fermi surface. If the zeros of the sine function, expressed as values of $1/H$, are plotted against successive integers, a graph of the
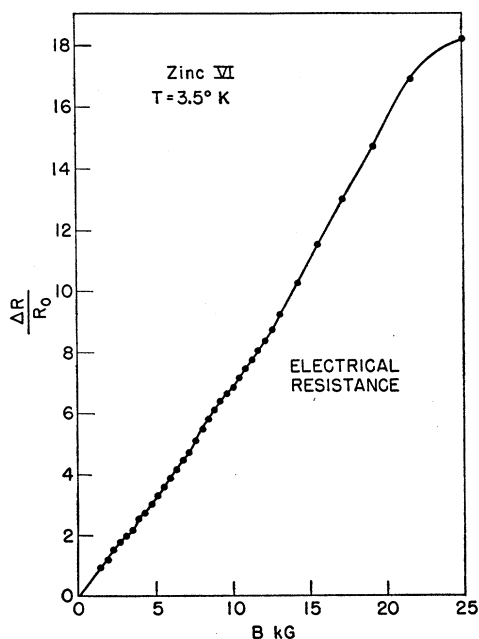

FIG. 7. Relative change in electrical resistance as a function of field for Zn VI. Hexagonal axis is perpendicular to current and parallel to field direction.

type shown in Fig. 9 is obtained. The slope of this line is equal to $\beta^*/2E_0$, and the ratio is usually broken, in the case of susceptibility measurements, by a study of the temperature dependence of the amplitude of the oscillations.

Values of β^*/E_0 obtained from the electrical and thermal measurements on Zn VI and Zn VII appear in Table II. The best value from susceptibility measurements is given for comparison.

DISCUSSION AND CONCLUSIONS

Comparison with Theory

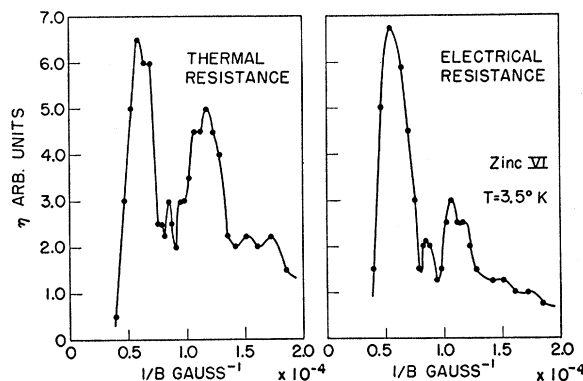Apart from the oscillatory effects, the magnetoresistive behavior of these specimens have been ana-

FIG. 8. Difference curves for thermal and electrical magnetoresistance of Zn VI, showing de Haas-van Alphen oscillations.

lyzed in the light of the 2-band theory of Sondheimer and Wilson,[12] first published in 1947 and somewhat amplified in the second edition of Wilson's *Theory of Metals*[13] in 1953. They consider a model consisting of two overlapping bands of electrons, the s-band and the d-band, whose energies are given by $E = \hbar k^2/2m$. The model is not claimed to be representative of any real metal, but was chosen for its mathematical tractability.

It yields equations of a familiar form:

$$\Delta\rho/\rho_0 = AH^2/(1+BH^2) \quad \text{(electrical)},$$

$$\Delta W/W_0 = CH^2/(1+DH^2) \quad \text{(thermal)}.$$

They describe a magnetoresistance curve which is parabolic at low fields and which approaches some constant value at high fields. If we assume that two bands make equal contribution to the conductivities, so that $\sigma_s = \sigma_d = \sigma_0/2$ and $K_s = K_d = K_0/2$, we can then determine the number of electrons in each band. For the
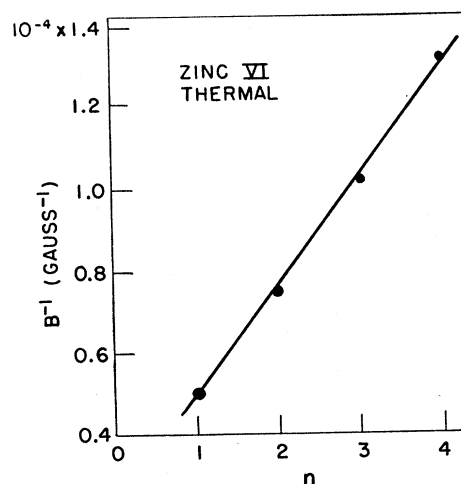

FIG. 9. Straight-line plot used to analyze de Haas-van Alphen oscillations found in thermal magnetoresistance of Zn VI.

[12] E. H. Sondheimer and A. H. Wilson, Proc. Roy. Soc. (London) 190, 435 (1947).
[13] A. H. Wilson, *Theory of Metals* (Cambridge University Press, Cambridge, 1953), second edition.
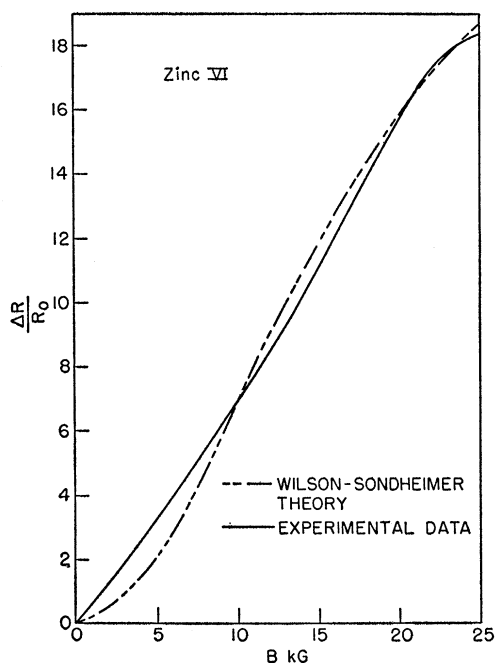
FIG. 10. Comparison of experimental results on the electrical magnetoresistance of Zn VI with the theory of Sondheimer and Wilson.

electrical case, the constants are

$$A = \frac{(n_s + n_d)^2}{(n_s n_d)^2} \left(\frac{\sigma_0}{4ec} \right)^2,$$

$$B = \frac{(n_s - n_d)^2}{(n_s n_d)^2} \left(\frac{\sigma_0}{4ec} \right)^2,$$

and for the thermal case

$$C = \frac{(n_s + n_d)^2}{(n_s n_d)^2} \left(\frac{3eK_0}{4\pi^2 k^2 cT} \right)^2,$$

$$D = \frac{(n_s - n_d)^2}{(n_s n_d)^2} \left(\frac{3eK_0}{4\pi^2 k^2 cT} \right)^2,$$

where n_s = number of electrons/cc in the s-band, n_d = number of electrons/cc in the d-band, σ_0 = electrical conductivity in zero field (gaussian units), e = electronic charge (esu), c = velocity of light (cm/sec), k = Boltzmann constant (erg/°K), K_0 = thermal conductivity

TABLE III. Values derived from Wilson-Sondheimer theory for the number of electrons in the s-band (n_s) and the number in the d-band (n_d). The number of electrons per atom for the respective bands is also shown.

Zn VI	n_s	n_d	n_s/atom	n_d/atom
Thermal	2.22×10²²	0.914×10²²	0.332	0.137
Electrical	1.70×10²²	1.12 ×10²²	0.255	0.168

in zero field (gaussian units), and T = absolute temperature. By taking the experimentally observed values of $\Delta\rho/\rho_0$ and $\Delta W/W_0$ at two fields, 10 kilogauss and 20 kilogauss, and substituting these in the equations quoted above, values of n_s and n_d can be determined for both the electrical and thermal cases. The results are shown in Table III. While a certain measure of agreement exists between the values derived in both cases, it should not be concluded that the experimental results agree with theoretical predictions. Figure 10 shows a comparison between theory and experiment, using the constants just derived. It is clear that the simple parabolic behavior predicted is not borne out at low temperatures, at least. However, a somewhat more fundamental discrepancy exists in the number of electrons per atom. It is considerably less than the number one would intuitively expect for a metal like zinc, although other experiments on thermal conductivity give similar results. The work of Webber, Andrews, and
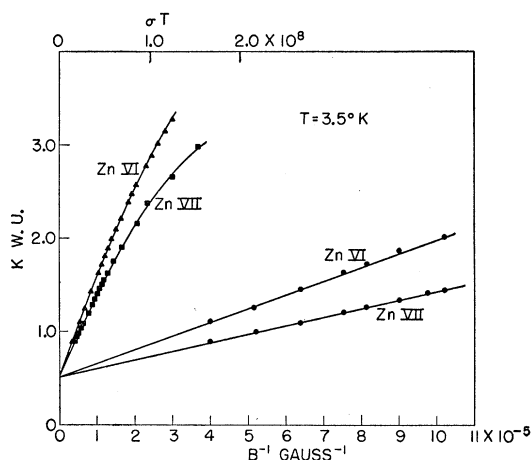

FIG. 11. Two methods of determining the value of thermal conductivity of Zn VI in very large fields (K_∞). The σT axis is used in conjunction with the two curves marked with squares (■) and triangles (▲). The K-intercept at $B^{-1} = 0$ is 0.50 watt units.

Spohr[14] for example, yielded a value of 6×10^{-2} electrons per atom for aluminum. In addition, the susceptibility measurements of the de Haas-van Alphen effect indicate that only about 1×10^{-6} electrons per atom are taking part in the oscillations. If we assume, from the size of the de Haas-van Alphen component, that only one percent of the total number of electrons taking part in the conduction process are de Haas-van Alphen electrons, we arrive at a figure of 1×10^{-4} electrons per atom. This is clearly much too small, but the qualitative fact remains that the number of electrons per atom available for thermal or electrical conduction at low temperatures is apparently an order of magnitude less than the valence number, two.

---

[14] Webber, Andrews, and Spohr, Phys. Rev. 84, 994 (1951).

Extrapolation to Infinite Fields

Two techniques have been employed to determine the value of the thermal magnetoresistance in an infinitely large field for Zn VI and Zn VII. The first is very straightforward; the data are expressed as thermal conductivity and then plotted against the reciprocal of the field. From about 10 kilogauss up, the experimental points fall on a reasonably good straight line which can be extrapolated to $1/H = 0$ or $H = \infty$. The point of intersection of this line with the K axis presumably gives the value to which the conductivity is tending.

The second method is similar to the first, except that instead of an abscissa of $1/H$, we use σT, the product of the electrical conductivity and the temperature. This has the effect of separating the thermal conductivity into two parts; one, a part designated K_e which depends on the same electrons as the electrical conductivity and thus is sensitive to a magnetic field, and the other, a field-independent part, designated K_∞. If we make the questionable assumption that in the limit of infinitely large H, σ goes to zero, the K-intercept gives the value of K_∞. The results of such an analysis appear in Fig. 11. The agreement between the values of K_∞ derived by the two methods is probably fortuitous; nevertheless, the fact that two different crystals yield the same result is intriguing.

If we assume that the thermal conductivity of the metallic lattice, K_g, can be added to the thermal conductivity of the electrons and that the electronic contribution is reduced to zero in the limit of large fields, it would seem that K_∞ could be identified with K_g. In fact, the second method given above is one of the techniques used to yield an estimate of K_g. For these experiments, however, this is apparently not the case. If we take the data for Zn I (A) and Zn I (B) and plot the values of thermal conductivity against reciprocal field (method 1), we obtain the curves shown in Fig. 12. It is clear that the values of K_∞ for the two cases are quite different, indicating that the angular anisotropy observed at ordinary fields persists for indefinitely large ones. This indicates that the electronic contribution to the thermal conductivity is never completely quenched by a magnetic field. It is probable that at very high fields, both the thermal and electrical conductivities reach a value which no longer depends on the magnitude of the field, but only on its direction with respect to the crystalline axes.

The Lorenz Ratio

The Lorenz ratio derived from these experiments is somewhat anomalous. If we calculate $L_0 = K_0/\sigma T$ from the data given in Table I, we see that it is considerably below the value to be expected at these temperatures. For Zn VI, $L_0 = 1.32 \times 10^{-8}$ and for Zn VII, $L_0 = 1.38 \times 10^{-8}$. The values obtained for other metals at these temperatures are usually much closer to the room temperature value of 2.45×10^{-8} watt-ohm/$(°K)^2$. In
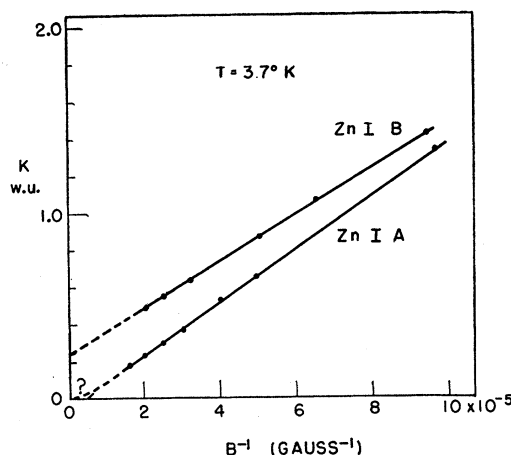

FIG. 12. Graph showing persistence of angular anisotropy in thermal conductivity at very high fields for Zn I.

addition, the variation of L with field is quite strong, indicating that the thermal and electrical conductivities are not mere reflections of each other. Figure 13 shows the variation of L/L_0 with field for Zn VI. Although L_0 is almost certainly in error, the data showing the relative change of L with field is probably valid. Using the values of n_s and n_d derived earlier and substituting into the expression for L/L_0 given by Wilson,[12]

$$\frac{L}{L_0} = \frac{1 + \frac{1}{8}\left(\frac{H}{ec}\right)^2 \left(\frac{n_s^2 + n_d^2}{n_s^2 n_d^2}\right)\sigma_0^2}{1 + \frac{1}{8}\left(\frac{H}{ec}\right)^2 \left(\frac{n_s^2 + n_d^2}{n_s^2 n_d^2}\right)\frac{L_0^2}{L_n^2}\sigma_0^2}$$

$$\frac{1 + \frac{1}{16}\left(\frac{H}{ec}\right)^2 \frac{(n_1 - n_2)^2}{n_1^2 n_2^2}\frac{L_0^2}{L_n^2}\sigma_0^2}{1 + \frac{1}{16}\left(\frac{H}{ec}\right)^2 \frac{(n_1 - n_2)^2}{n_1^2 n_2^2}\sigma_0^2},$$
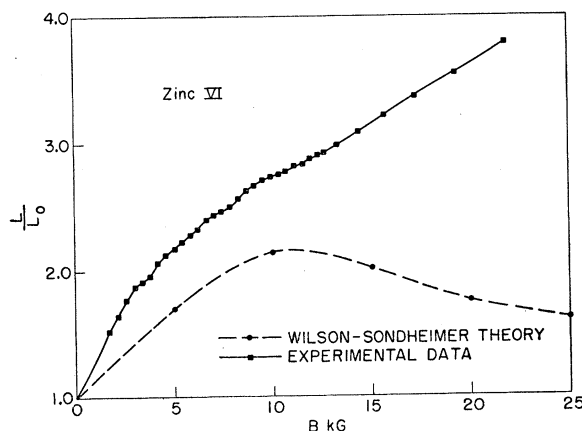
we have the result shown in dotted lines in Fig. 13.

FIG. 13. Comparison of experimental results on the Lorenz ratio of Zn VI with the theoretical results of Sondheimer and Wilson.

ACKNOWLEDGMENTS

Absorption of Light by Atoms in Solids*

D. L. DEXTER

Institute of Optics, University of Rochester, Rochester, New York and United States Naval Research Laboratory, Washington, D. C.

(Received September 16, 1955)

The interactions of an atom with its neighbors in an idealized solid are taken into account explicitly in treating the absorption of light, as contrasted with the usual introduction of an "effective" field and mass. In the discussion of the magnitude of the absorption coefficient, two cases are treated: one, the absorption by an impurity atom, in which case we are led to an equation similar to Smakula's; and two, the absorption by one of the atoms of the perfect crystal. The computations are based on a simple idealized model whose validity is discussed for existing systems.

I. INTRODUCTION

CONSIDERABLE progress has been made in recent years in the understanding of the shape of absorption bands of atoms in solids, particularly of impurity atoms.[1-5] Relatively little attention has been directed to the problem of the total amount of absorption by the atom, that is, to the integrated cross section. This is a somewhat more difficult problem, requiring explicit knowledge of the details of the wave functions, which are, in most cases, severely modified by the medium from their values *in vacuo*.

The usual method[2] for the treatment of the magnitude of the absorption has been to make use of the atomic wave functions of the atom, completely uninfluenced by the presence of the medium, and to attempt to take account of the effect of the medium by the introduction of an "effective field" and an "effective mass" for the electron. This procedure is satisfactory in limiting cases, where the values of these effective parameters are known, but suffers from the difficulty that in general the parameters are not known. In an alternative description, presented here, the transition probability of the system is calculated, using wave functions for the whole crystal in which interactions among the atoms are taken into account. Since the interactions are explicitly accounted for in the wave functions, the introduction of effective masses and fields is unnecessary, and this difficulty is avoided; for this difficulty there is substituted the problem of calculating wave functions in which the interactions are included. This is, in general, a formidable task since the interactions are many and large, so large, in fact, that perturbation theory may not be applicable in a simple way in some systems.

In one idealized model, however, the calculation of the wave functions and the transition probability can easily be carried out, and the results can be expressed in a form similar to Smakula's equation[6,7] for impurity atom absorption. This is included in Sec. II, where there is also presented a discussion of the simplifying assumptions inherent in the idealized model. In Sec. III is a similar calculation for the absorption of the pure host crystal itself. In this case we obtain a result, not previously emphasized to the knowledge of the writer, which is equivalent to the statement that the integrated absorption cross section of an oscillator is unchanged by the dipole-dipole interactions with other identical oscillators.

II. IMPURITY ABSORPTION

Here we shall be concerned particularly with an impurity atom which absorbs light of a longer wavelength than that at which the host crystal absorbs; thus its absorption is not lost in the fundamental absorption of the host crystal. We shall also assume that the impurity concentration is sufficiently low, say less than

* This research was supported in part by the U. S. Air Force through the Office of Scientific Research of the Air Research and Development Command.

[1] K. Huang and A. Rhys. Proc. Roy. Soc. (London) **A204**, 406 (1950).

[2] M. Lax, J. Chem. Phys. **20**, 1752 (1952) and subsequent publications.

[3] F. E. Williams, J. Chem. Phys. **19**, 457 (1951) and subsequent publications.

[4] C. C. Klick, Phys. Rev. **85**, 154 (1952).

[5] D. L. Dexter, Phys. Rev. **96**, 615 (1954).

[6] A. Smakula, Z. Physik **59**, 603 (1930).

[7] C. Herring, Proceedings of the Atlantic City Conference on Photoconductivity, November, 1954 (John Wiley and Sons, Inc., New York, 1955). Herring has suggested some modifications to Smakula's equation based on a somewhat different point of view than that expressed here.